



1 **Testing the validity of regional detail in global analyses of Sea**  
2 **surface temperature — the case of Chinese coastal waters**

3 Yan Li<sup>1\*</sup>, Hans von Storch<sup>2,3</sup>, Qingyuan Wang<sup>4</sup> and Qingliang Zhou<sup>5</sup>

4 <sup>1</sup>National Marine Data and Information Service, Tianjin, People's Republic of China

5 <sup>2</sup>Institut für Küstenforschung, Helmholtz zentrum Geesthacht, Germany

6 <sup>3</sup>Ocean University of China, Qingdao, People's Republic of China

7 <sup>4</sup>Tianjin Meteorological Observatory, Tianjin, People's Republic of China

8 <sup>5</sup>Chinese Meteorological Administration, Beijing, People's Republic of China

9

10 **Abstract.** We have designed a method for testing the quality of multidecadal analyses of SST  
11 in regional seas by using a set of high-quality local SST observations. In recognizing that  
12 local data may reflect local effects, we focus on dominant EOFs of the local data and of the  
13 localized data of the analyses. We examine patterns, and the variability as well as the trends of  
14 the principal components. This method is applied to examine four different SST analyses,  
15 namely HadISST1, ERSST, COBE SST, and NOAA OISST. They are assessed using a newly  
16 constructed high-quality data set of SST at 26 coastal stations along the Chinese coast in  
17 1960-2015 which underwent careful examination with respect to quality, and a number of  
18 corrections of inhomogeneities. The four gridded analyses perform by and large well, in  
19 particular since 1980. However, for the pre-satellite time period, before 1980, the analyses  
20 differ among each other and show some inconsistencies with the local data, such as artificial  
21 break points, periods of bias and differences in trends. We conclude that gridded SST-analyses  
22 need improvement in the pre-satellite time (prior to 1980s), by re-examining in detail archives  
23 of local quality-controlled SST data in many data-sparse regions of the world.

24

---

\* Corresponding author. E-mail address: [ly\\_nmdis@163.com](mailto:ly_nmdis@163.com)



## 25 1. Introduction

26 Sea surface temperature (SST) is a key parameter for climate change assessments. It is  
27 significantly associated with many atmospheric and oceanographic modes, such as Pacific  
28 Decadal Oscillation (PDO), El Niño/Southern Oscillation (ENSO), Indian Ocean Dipole (IOD),  
29 etc. (Saji et al., 1999, Mantua and Hare, 2002, Yeh and Kim, 2010). A number of extended  
30 historical observed SST products have been used in global climatological community  
31 (Boehme et al. 2014; Hirahara et al. 2014), as well as in the regional climate change, for  
32 example the China Seas, the Baltic Sea and North Sea (Belkin, 2009; Wu et al., 2012;  
33 Stramska and Bialogrodzka, 2015). However, historical SST datasets have large uncertainties  
34 in long-term trend patterns in some regions. For example, observed SST changes in the  
35 tropical Pacific are still controversial, depending on the different dataset and study period  
36 (Bunge & Clarke 2009). Vecchiga et al. (2008) indicate that the equatorial zonal SST gradient  
37 in the Pacific has intensified in Hadley Centre Sea Ice and Sea Surface Temperature  
38 (HadISST) but weakened in Extended Reconstructed SST (ERSST) from the nineteenth to  
39 twentieth centuries. Scientists utilized several different datasets, including the reconstructed  
40 and un-interpolated datasets, to study the SST variability in tropical area and the China Seas  
41 (Xie et al., 2010; Liu and Zhang 2013, Tokinaga et al., 2012). They found that there were  
42 larger uncertainties in estimate of SST warming patterns using different SST datasets. Thus, it  
43 is also necessary for comparing different SST products over the regional areas in detail.

44 Coastal marine ecosystems yield nearly half of the earth's total ecosystem goods and services  
45 (Costanza, 1997). Simultaneously, they are highly influenced by local factors, such as the  
46 anthropogenic land-based processes, fresh water discharge and local tidal mixing. An accurate  
47 assessment of the local SST variability is needed most in marine ecosystem-based  
48 management. Here, we mainly focus on three globally gridded SST datasets, that is, the  
49 HadISST1, ERSST, COBE SST (Rayner et al., 2003, Ishii et al., 2005, Smith et al., 2008,  
50 Hirahara et al., 2014). All of these datasets have been widely used in the regional and global  
51 climate change studies. In order to test the validity of gridded SST datasets on a coastal scale,  
52 SST records for the period of 1960-2015 at total 26 coastal hydrological stations along  
53 Chinese coast are used which have been homogenized by adjusting artificial breakpoints. We  
54 study the performance of these gridded SST datasets in the coastal waters by comparing to the  
55 in situ SST records which have been homogenized.

56 Thus, the remainder of this paper is structured as follows: Details on the observational and  
57 gridded data sets and methodology used in this study are given in Section 2. Section 3



58 introduces the local homogenized SST time series along the Chinese coast (Li et al., 2018),  
 59 which is used as a reference to compare the gridded data to. For adding confidence in the  
 60 quality of this data set, these data are compared to independent data set of local air  
 61 temperature data. The basic statistics of the local SST-data series are shown. Section 4  
 62 describes the results and comparisons with gridded SST datasets in the Chinese coastal waters.  
 63 Further discussion and conclusion are given in Section 5.

## 64 2. Data and methodology

### 65 2.1. Data source

66 The SST records during 1960-2015 at the 26 sites of coastal hydrological stations along the  
 67 Chinese coast have been assembled and homogenized, using meta data and the Penalized  
 68 Maximal  $t$  (PMT) test (Li et al., 2018). Homogenized monthly mean surface air temperature  
 69 (SAT) series from National Meteorological Information Center (NMIC) of China (Xu et al.,  
 70 2013) and the gridded SAT from the latest version of the Climate Research Unit's (CRU)  
 71 gridded high resolution ( $0.5^\circ \times 0.5^\circ$ ) dataset CRU TS 3.24.01 for 1960-2015 (Harris et al.,  
 72 2014) are used to investigate the consistency of homogenized SST data with the local SAT.

73 Four globally gridded SST datasets are used (see Table 1): (1) The  $1^\circ \times 1^\circ$  Hadley Center Sea  
 74 Ice and Sea Surface Temperature monthly dataset (HadISST) (Rayner et al., 2003); (2) The  
 75  $1^\circ \times 1^\circ$  Centennial In Situ Observation-Based Estimates of the Variability of SST (COBE SST)  
 76 (Hirahara et al., 2014); (3)  $2^\circ \times 2^\circ$  Extended Reconstructed Sea Surface Temperature version 4  
 77 (ERSST v4) for 1960-2015 (Smith et al., 2008). (4) NOAA Optimum Interpolation SST  
 78 (OISST) version 2 with high spatial resolution of  $0.25^\circ \times 0.25^\circ$  for 1982-2015 (Reynolds et al.  
 79 2007).

80 **Table 1.** Global gridded SST datasets that are commonly used for climate studies

Dataset	Resolution	Period	Sources
ERSST v4	$2^\circ \times 2^\circ$	1960-2015	<a href="http://www.ncdc.noaa.gov/oa/climate/research/sst/ERSST.v4.php">http://www.ncdc.noaa.gov/oa/climate/research/sst/ERSST.v4.php</a>
HadISST	$1^\circ \times 1^\circ$	1960-2015	<a href="http://www.metoffice.gov.uk/hadobs/hadisst/data/download.html">http://www.metoffice.gov.uk/hadobs/hadisst/data/download.html</a>
COBE SST	$1^\circ \times 1^\circ$	1960-2015	<a href="http://ds.data.jma.go.jp/tcc/tcc/products/el_nino/cobesst/cobe-sst.html">http://ds.data.jma.go.jp/tcc/tcc/products/el_nino/cobesst/cobe-sst.html</a>
OISST	$\frac{1}{4}^\circ \times \frac{1}{4}^\circ$	1982-2015	<a href="http://www.esrl.noaa.gov/psd/data/gridded/data.noaa.oisst.v2.html">http://www.esrl.noaa.gov/psd/data/gridded/data.noaa.oisst.v2.html</a>

### 81 2.2. Methodology

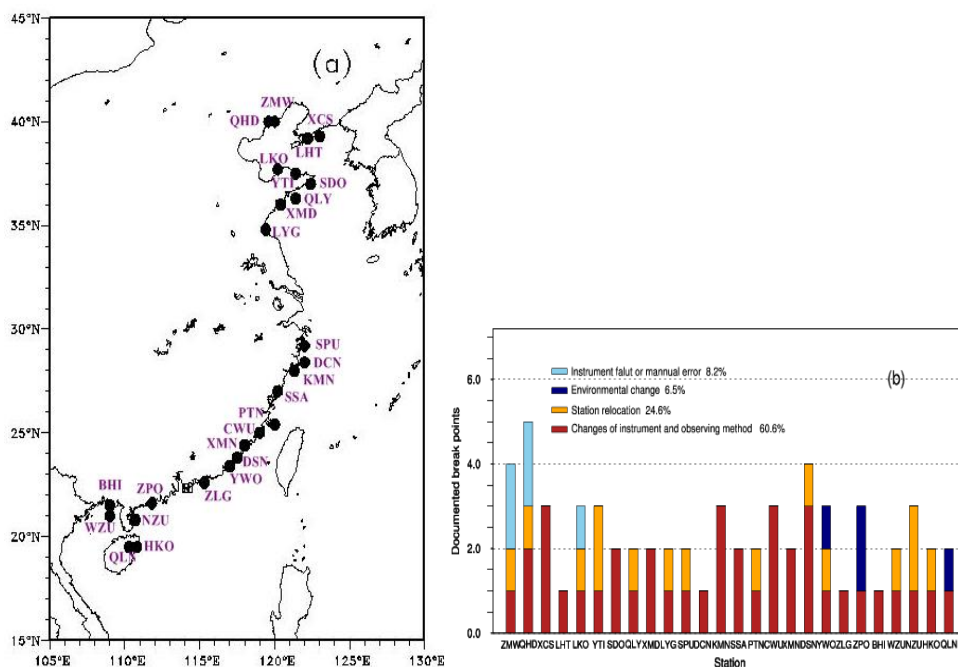


82 Statistical methods such as conventional empirical orthogonal function (EOF) (Kim et al.,  
83 1996, von Storch and Zwiers 1999), correlation analysis and linear trend analysis are  
84 performed. The significance of each trend has been tested with the Mann-Kendall test using  
85 Sen's slope estimates quantify trends (Sen, 1968). The tests were stipulated to operate with a  
86 probability for a false rejection of the null hypotheses (i.e., zero trend) of 5%. They are  
87 conducted with the implicit assumption that the data are serially independent. There are only  
88 weakly correlated but not really independent. Thus, the tests are “liberal”, i.e., have  
89 tendencies for falsely rejecting too often the null hypothesis, when it is actually valid (von  
90 Storch and Zwiers, 1999). However, since the effect is relatively weak, given the small serial  
91 correlations, and since we have no results, which are close to the stipulated critical levels, we  
92 do as if the serial dependence is not of importance. However, this caveat should be kept in  
93 mind, when assessing the results.

### 94 3. The local homogenized SST records along the Chinese coast

95 The locations of the 26 coastal hydrological stations and the identified break points at each  
96 station are displayed in Fig. 1a and 1b. The majority of change points are caused by  
97 instrument change and station relocation, accounting for about 60.6% and 24.6% of the total  
98 change points. In our work, we consider annual mean values. Some analyses with seasonal  
99 mean values are also calculated, but these are not covered by our present account and merely  
100 summarized. The supporting evidences are provided by the Supplementary Online Material  
101 (SOM) in Appendix B.

102 The standard statistics derived from the data in the period of 1960-2015, that is, long-term  
103 mean, the standard deviation of annual means and the decadal trends are listed in Table 2.  
104 SSTs vary spatially along the Chinese coast, between about 11.5 °C in the north and 25 °C in  
105 the far south. The standard deviations are of the order of 0.50 °C throughout, with a maximum  
106 of 0.71 °C and a minimum of 0.43 °C. The decadal trends vary between 0.13 °C per decade to  
107 0.29 °C per decade. Table 1 also provides the long-term means of the homogenized data and  
108 of the raw (unhomogenized) data. The differences between the homogenized data and the raw  
109 data (last column) vary between -2.26 °C and 0.53 °C. At most of the 26 stations, a downward  
110 correction has been found necessary – only at two stations (YWO and PTN) an upward  
111 change was stipulated, in one case no change of the mean and in the remaining 23 a  
112 downward or zero change.



113

114 **Figure 1.** Locations of 26 coastal sites(a), for which continuous monthly SST recordings are available and  
 115 corrected by eliminating inhomogeneities. The identified breakpoints in individual SST stations from 1960-  
 116 2015(b).Results from Li et al. 2018.

117

118 **Table 2.** Statistics of the time series of the annual local homogenized SST, plus the differences to the raw  
 119 data, which were used to construct the homogenized series (columns 7 and 8).

Station No.	Station name	Abbreviation	Mean Homogenized SST	Standard deviation	Trend (°C/10yrs)	Mean unhomogenized SST	Diff
1	Zhi Maowan	ZMW	11.50	0.53	0.17	11.75	-0.25
2	Qin Huangdao	QHD	12.21	0.59	0.26	12.32	-0.11
3	Xiao Changshan	XCS	11.54	0.71	0.29	11.73	-0.19
4	Lao Hutun	LHT	11.36	0.59	0.21	11.47	-0.11
5	Longkou	LKO	13.36	0.59	0.22	13.51	-0.15
6	Yantai	YTI	12.65	0.59	0.17	12.79	-0.14
7	Shidao	SDO	12.09	0.59	0.14	12.08	0.01
8	Qian Liyan	QLY	14.37	0.65	0.17	14.41	-0.04
9	Xiao Maida	XMD	13.76	0.63	0.22	13.84	-0.08



10	Lian Yungang	LYG	14.85	0.57	0.21	14.94	-0.08
11	Shipu	SPU	17.41	0.65	0.26	18.01	-0.61
12	Dachen	DCN	17.67	0.65	0.24	17.91	-0.24
13	Kanmen	KMN	18.20	0.56	0.17	18.42	-0.22
14	Sansha	SSA	19.21	0.71	0.21	19.91	-0.19
15	Pingtang	PTN	19.72	0.61	0.19	19.45	0.53
16	Congwu	CWU	19.98	0.52	0.17	22.18	-0.64
17	Xiamen	XMN	21.50	0.51	0.19	21.47	-2.26
18	Dongshan	DSN	20.84	0.45	0.13	21.12	-0.28
19	Yunwo	YWO	21.02	0.44	0.13	21.36	-0.34
20	Zhelang	ZLG	22.43	0.44	0.15	22.62	-0.19
21	Zhapo	ZPO	23.62	0.50	0.18	23.68	-0.06
22	Beihai	BHI	23.60	0.55	0.18	24.06	-0.46
23	Weizhou	WZU	25.79	0.43	0.17	25.66	0.13
24	Naozhou	NZU	24.46	0.49	0.16	24.44	0.02
25	Haikou	HKO	25.00	0.49	0.16	25.10	-0.10
26	Qinglan	QLN	25.80	0.44	0.18	25.86	-0.07

120

121 The quality of the data set has already been documented by Li et al., 2018; to add confidence  
 122 in the quality of this data set, we compared the new data set to an independent data set of 26  
 123 local surface air temperature (SAT). Also, this data set has been homogenized - independently  
 124 of the processing of the SST series. We find the SST series fully consistent with these SAT  
 125 series, as well as with the gridded CRU data (not shown, see Appendix A). Thus, we conclude  
 126 that our data set is superior to earlier used data on the SST variability and trends along the  
 127 Chinese coast.

#### 128 4. Comparison with gridded SST datasets in the Chinese coast waters

129 After we have found the newly homogenized SST series consistent with independent regional  
 130 data, we use them as a benchmark for assessing the regional quality of the four globally  
 131 gridded SST datasets (Table 1). In the following, we name the new dataset “Local  
 132 homogenized SST-analysis” and refer to it as LH, while the datasets extracted from the  
 133 gridded SST datasets as “localized analysis data”, and use the abbreviation LA. For instance,  
 134 LA-HadISST is the data set of SST found in the dataset HadISST in that grid box, which  
 135 contains the locations in the LH data set.

136 These “localized” time series (LA) of the three gridded datasets, which extend to the full time  
 137 window 1960-2015 (ERSST, HadISST, COBE SST,; referred as LA-ERSST, LA-HadISST,



138 LA-COBE SST) are then compared to the local series — LH, by first comparing the standard  
139 deviations and the trends, and by calculating from trends, differences (Diff) and the root mean  
140 square errors (RMSEs) for the 26 stations (see Table 3). We do this for annual mean values.  
141 The fourth dataset, OISST data, covers a shorter time window from 1982-2015. It is used in  
142 the concluding section for clarifying some additional aspects in the section 5.

143 For summarizing the results, we again compute EOFs of the LH and the LAs, as well as for  
144 the differences of LH and LAs. The LH data are derived from observational stations, whereas  
145 the LA data are representing area values averaged across a grid box. Therefore, the LA data  
146 should vary less than the LH data. Possible mismatches between the local (point) LH data and  
147 the spatial averages of grid box data in the LAs may be related to small scale effects; however,  
148 the usage of EOFs is expected to reduce these truly local specifics, as the first EOFs describe  
149 joint co-variations among the 26 elements in both LA and LH data sets.

#### 150 4.1. Comparing with HadISST

151 The 56-year mean values of local SST in the analysis LA-HadISST are in all cases higher than  
152 at the local stations (Table 3). Some differences are of the order of 2 °C and even 3 °C, in  
153 particular along the East China Sea extending from SPU to ZLG (stations No. 11-20; see  
154 Fig.1). To some extent, this difference may reflect differences between averages of a larger  
155 coastal ocean area and *in situ* observations, but not entirely.

156 The variations in LA are similar to LH, but there are some differences: as expected, the  
157 standard deviations are in most cases (17) larger for LH, and only in few cases (9) smaller.  
158 The correlations are all large enough to reject the null hypothesis of the absence of a link (if  
159 we assume serially independence the 90%-critical value is 0.22) except for the northernmost  
160 station YWO. Part of the difference to the ideal value of 1 may be due to the different spatial  
161 scale, but values as low as 0.41 allude to more systematic differences. The trends are positive  
162 for all sites (Table 3) – only the northernmost station ZMW signals a weak downward trend in  
163 the LA-HadISST data set. In about 50% of the case, the coastal sea warms faster according to  
164 LH than according to LA-HadISST, and for 50% it is the opposite. For the two northernmost  
165 sites, ZMW and QHD station, the warming according to LA is very weak, whereas along the  
166 stretch from PTM to YWO the warming according to LA-HadISST is considerably stronger  
167 than in LH.

168 The time series for the two northern sites in the Bohai Sea are shown in Fig. 2. The sequence  
169 of maxima and minima share some similarity, but the trends differ markedly. The LH curves



170 (red lines) exhibit both a steady increase, whereas the LA-HadISST curves (black lines) tend  
 171 to decline in the first 10-20 years, and to vary at a mostly constant level (Fig.2a and 2b). In  
 172 this case, the “story told” by LH is considerably different than that of LA-HadISST. The time  
 173 series of the SST averaged across the stations from PTN to YWO along the East China Sea  
 174 coast, where LA-HadISST indicate a stronger warming than in the LH, is shown in Fig. 2c.  
 175 The local data indicate markedly lower temperatures, which may reflect by local effects, but  
 176 also a weaker trend (0.18 °C per decade) than in the LA-HadISST (0.35 °C per decade).

177 **Table 3.** Statistics of the time series of the localized SST-analysis (LA-HadISST) data series at the 26  
 178 station, as well as the differences (Diff) between statistics of the LH series given in Table 1. The correlation  
 179 coefficients between LH and LA-HadISST are also calculated (the 90% confidence level is 0.22, without  
 180 considering serial correlation). Red numbers indicate that the correlation coefficients do not conflict with  
 181 the null hypothesis of no correlation.

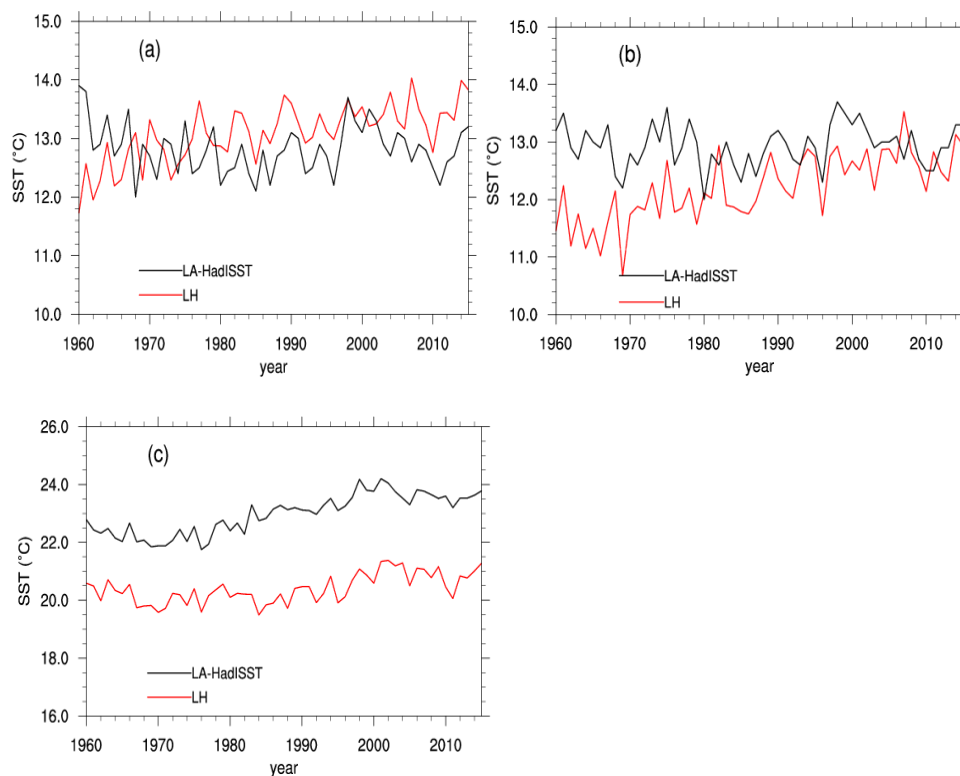
Station No.	Station	Mean LA-HadISST	Diff	Std deviation LA-HadISST	Diff	Trend (°C/10yrs)	Diff	Corr
1	ZMW	12.80	-1.32	0.43	-0.06	-0.02	0.25	<b>0.20</b>
2	QHD	12.93	-0.72	0.37	0.21	0.02	0.24	0.31
3	XCS	13.45	-1.76	0.46	0.38	0.13	0.16	0.73
4	LHT	13.86	-2.30	0.51	0.07	0.15	0.07	0.67
5	LKO	13.71	-0.24	0.54	0.28	0.11	0.11	0.66
6	YTI	13.92	-1.12	0.57	0.01	0.14	0.03	0.69
7	SDO	14.87	-2.58	0.58	0.01	0.19	-0.05	0.70
8	QLY	14.51	0.01	0.54	0.10	0.14	0.03	0.77
9	XMD	14.51	-0.60	0.54	0.08	0.14	0.08	0.66
10	LYG	16.05	-1.07	0.47	0.10	0.21	0.00	0.71
11	SPU	19.70	-2.00	0.57	0.08	0.12	0.14	0.63
12	DCN	20.66	-2.65	0.59	0.05	0.27	-0.03	0.67
13	KMN	20.66	-2.12	0.59	-0.03	0.27	-0.10	0.64
14	SSA	22.47	-2.30	0.70	0.01	0.35	-0.14	0.73
15	PTN	23.43	-3.00	0.75	-0.14	0.34	-0.15	0.65





16	CWU	23.43	-1.45	0.77	-0.25	0.40	-0.23	0.75
17	XMN	22.03	-2.41	0.77	-0.26	0.40	-0.21	0.78
18	DSN	24.46	-3.26	0.59	-0.14	0.30	-0.17	0.59
19	YWO	24.46	-3.08	0.59	-0.15	0.30	-0.17	0.66
20	ZLG	25.44	-2.82	0.46	-0.02	0.20	-0.05	0.83
21	ZPO	25.66	-1.78	0.51	-0.01	0.07	0.11	0.56
22	BHI	25.11	-1.47	0.31	0.24	0.07	0.11	0.53
23	WZU	25.11	0.71	0.31	0.13	0.07	0.10	0.41
24	NZU	25.65	-1.02	0.40	0.09	0.19	-0.03	0.55
25	HKO	25.65	-0.47	0.40	0.09	0.19	-0.03	0.57
26	QLN	25.93	0.09	0.43	0.00	0.22	-0.04	0.64

182



183

184

185 **Figure 2.** The annual mean SST series of LA-HadISST (black line) and LH (red line) from ZMW station (a)  
186 and QHD station (b); The averaged annual mean SST series of LA-HadISST (black line) and LH (red line)  
187 from PTN station to YWO station (c).

188

189 The first two EOFs of the LH and the LA data set have similar patterns, namely a uniform  
190 sign along the entire coast in EOF1, with similar intensities, and a north-south dipole (Bohai  
191 Sea and Yellow Sea vs. East and south China Sea), with a sign change at SPU for the second  
192 (Fig.3a and 3b). The two patterns of LH explain less, namely 82.9% of the total variance, than  
193 the LA-HadISST EOFs, which go with 92.9%. This may be related to the larger spatial  
194 variability in local data compared to gridded data. In EOF1, again the two stations QHD and  
195 ZMW in the Bohai Sea contribute less in LA-HadISST, whereas the stations PTN to YWO  
196 contribute more to the overall warming than in LA-HadISST than in LH.

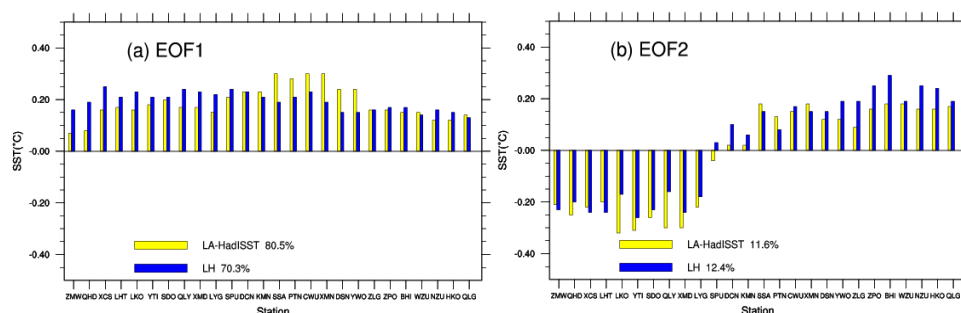
197 The time coefficients (PCs) are broadly similar, even if the correlations are not very strong:  
198 only 0.84 and 0.42 (Fig.3c and 3d). A general warming is associated with EOF1 and mostly  
199 stationary inter-annual variability with EOF2. Again, the sequence of maxima and minima is



200 qualitatively similar, but PC2 of LA-HadISST exhibits a break point at about 1980 –  
201 interestingly the time when satellites became routinely available of the global analyses.  
202 Before 1980, PC2 of LH and LA-HadISST differed by about 0.2 °C (Fig. 3d; this corresponds  
203 to a mean difference of 0.04 °C at the southern stations during that time, and a mean difference  
204 0.04 °C at the northern stations (Fig. 3b)).

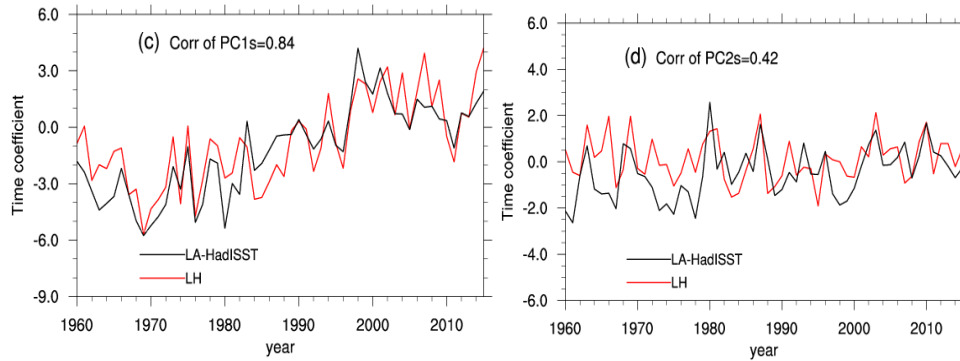
205 To further study the differences in trends, EOFs were calculated from the difference time  
206 series, that is, LH anomalies minus LA-HadISST anomalies at the 26 sites (Fig. 4). The first  
207 two EOFs stand for 31.2% and 27.6% of the variance. These numbers are not very different,  
208 and their closeness may be indicative that the EOFs are degenerate (von Storch & Zwiers  
209 1999). These EOFs describe covariations of the differences along long stretches of the coast;  
210 in case of EOF1, this is the case for all stations south of SPU, i.e., in the East and South China  
211 Sea (Fig.4a). In EOF2 it is all stations south of KMN, mostly in the Yellow Sea and Bohai Sea  
212 (Fig. 4b). PC1 seems to describe a change point at about 1980, whereas PC2 describes a slight  
213 upward trend: The difference time series tend to be larger in earlier years and are almost nil in  
214 the end of the considered time interval. That is, in recent years, there are little differences  
215 between LA-HadISST and LH, which is not surprising giving the better observational and  
216 reporting practice.

217 That in early years inhomogeneities impacted the quality of SST analyses is also not  
218 surprising, but it is valuable to learn when these inhomogeneities took place, and which time  
219 periods in the analyses should be taken with some reservation. Of course, this assertion  
220 depends on the assumption that the homogenization of the local data did remove all break  
221 points and other inhomogeneities.



222

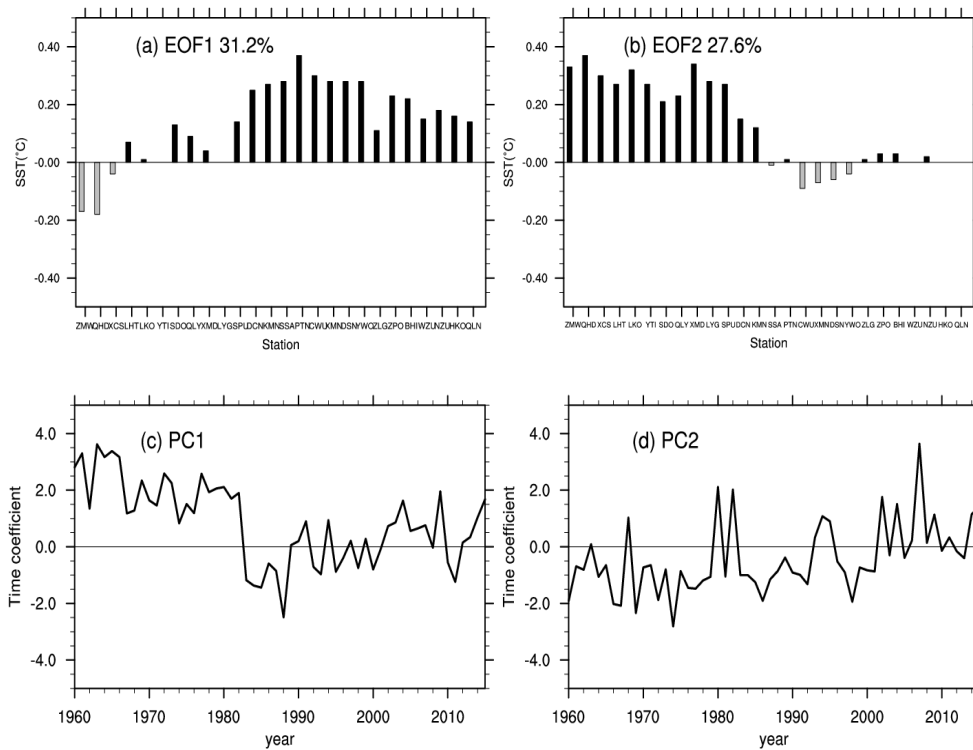
223



224

225 **Figure 3.** Comparison of the EOF1 and EOF2 derived from the LH data set of local SST at 26 sites (blue  
 226 bars; red lines), and derived from the localized analysis data LA-HadISST (yellow bars; black lines).  
 227 Top: EOF spatial patterns, bottom: principal components (time coefficients).

228



229

230

231 **Figure 4.** First two EOFs of the difference time series LH-LA-HadISST. Top: EOF spatial patterns, bottom:  
 232 principal components (time coefficients).

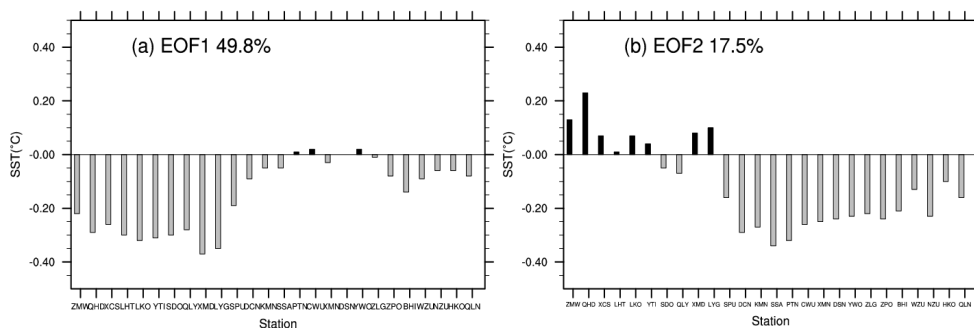
233



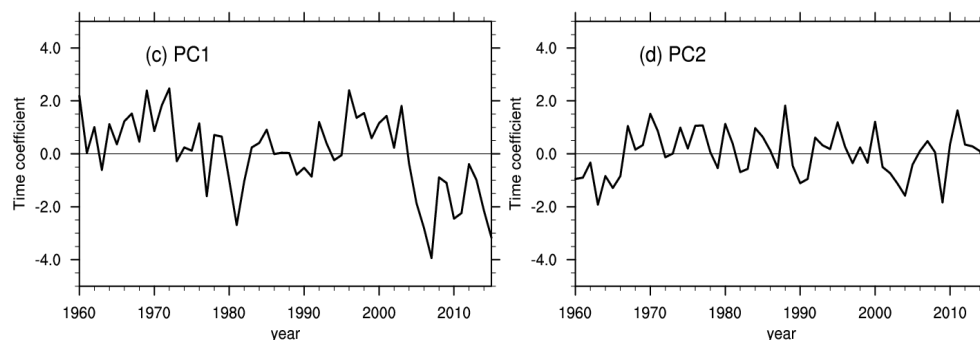
#### 234 4.2 Comparing with COBE SST

235 In this subsection, we consider the localized SST derived from the LA-COBE SST data set  
236 during 1960-2015. Again, the LA-COBE SST is in almost all sites higher than the local data,  
237 namely at 21 out of 26 sites. The differences are up to 3 °C, and again mostly along the East  
238 China Sea coast from SPU to ZLG (not shown, see Table SOM-1 in the Supplementary  
239 Online Material (SOM)). The local correlations are relatively high, namely between 0.55 and  
240 0.85. The EOFs derived from the LA-COBE SST, with the same grid resolution of 1°, and the  
241 same time window 1960-2015, as LA-HadISST exhibits broadly the same pattern in space  
242 and time as the EOFs of the LH data. Also, the explained variances are close (not shown, see  
243 Figure SOM-2). When comparing details, the northern stations contribute more to the overall  
244 warming represented by EOF1, whereas the stations along the South and East China Sea  
245 contribute less. Again, the two northernmost stations ZMW and QHD exhibit some systematic  
246 differences, both in EOF1 and EOF2. The PCs share correlations of 0.80 for EOF1 and 0.50  
247 for EOF2. COBE SST does not capture the recovery of the dip in warming since about 2000,  
248 as LH and HadISST did, while EOF2 reveals some warming in the final years. During the  
249 1960s some differences prevail.

250 Fig.5 shows the EOFs of the difference time series between LH anomalies and LA-COBE  
251 SST anomalies. The first EOF dominates, with 49.8%, whereas the second one represents a  
252 share of 17.5%. The first EOF points to several inhomogeneities, with two prolonged intervals  
253 during which LH is higher than LA-COBE SST (say, 1960-1978, and 1995-2005), and a  
254 strong drop-down to negative PC-values after about 2005. PC2, on the other hand, appears as  
255 mostly stationary, except for a suspiciously negative episode in the early 1960s.



256



257

258 **Figure 5.** EOF analysis of the differences LH-LA-COBE: Top: EOF spatial patterns (EOFs), bottom:  
259 principal components (time coefficients).

### 260 4.3 Comparing with ERSST

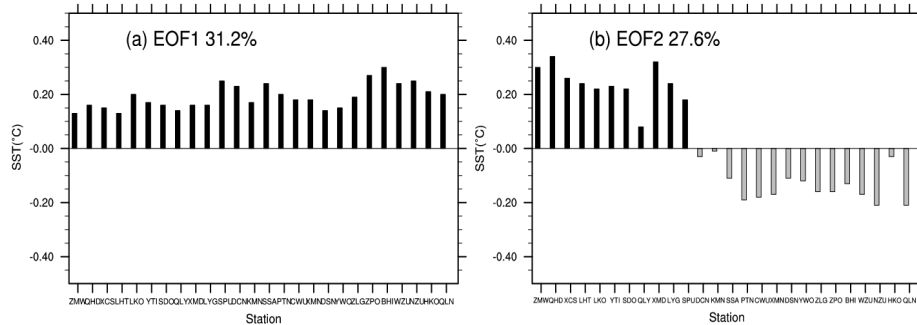
261 ERSST presents SST on a coarser grid compared to the two cases before, namely  $2^\circ$  by  $2^\circ$ .  
262 Again, the temperatures given by ERSST, as was the case with the other two analyses, is  
263 higher than the temperatures recorded at the local sites along the coast (not shown; see Table  
264 SOM-2). The differences are up to  $4^\circ$ , and the largest differences are found in the East China  
265 Sea from SPU to ZLG. That the differences are in this case even larger than in the other LA  
266 cases may be related to the  $2^\circ$  resolution of ERSST.

267 The variability according to ERSST is quite similar to that of LH, at least in terms of EOFs  
268 (not shown; see Figure SOM-3). The correlation of the PC1 is amount to 0.83, and of PC2 to  
269 0.60. LA-HadISST got 0.84 and 0.42, LA-COBE SST got 0.80 and 0.50. The local  
270 correlations vary between 0.37 and 0.82. Again EOF1 stands for an overall warming and  
271 EOF2 to interannual variability with hardly a trend. The relative contributions of the two  
272 EOFs compare well to the LH-EOFs. In detail, the northernmost stations appear stronger in  
273 EOF1 of LA-ERSST than in that of LH, whereas the northern sites are underrepresented, and  
274 the southern over-represented in EOF2.

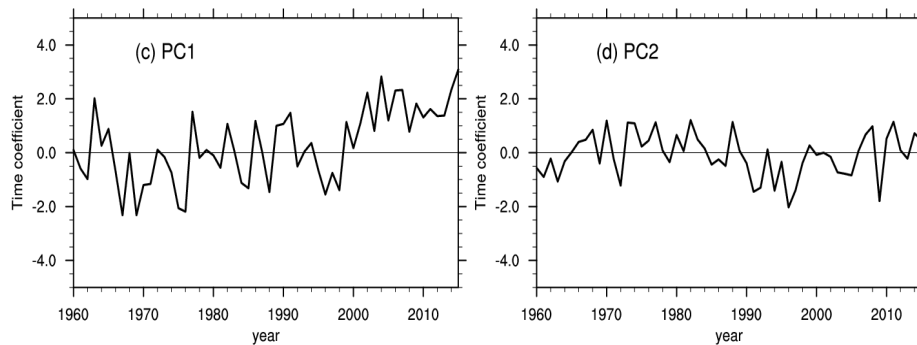
275 The EOFs of the differences between LH anomalies and LA-ERSST anomalies are shown in  
276 Fig. 6. They differ strongly from those found for LA-COBE SST and LA-HadISST. The first  
277 EOF differences resemble the first EOFs of LH and LA-ERSST (not shown; see Fig. SOM-3)  
278 – the long-term trend in LA-ERSST is smaller than in the local data – everywhere. The  
279 second EOF is again a dipole pattern, with the Yellow Sea and Bohai Sea on the one side, and  
280 the East and South China Sea on the other. PC2 is mostly stationary.



281



282



283 **Figure 6.** Spatial variability of the EOF1 (a); EOF2 (b) mode of the differences between LH anomalies and  
284 LA-ERSST anomalies (LH anomalies minus LA-ERSST anomalies). And the time coefficient series of  
285 PC1(c) and PC2 (d) from 1960 to 2015.

286

## 287 5 Discussion and conclusion

288 We have mainly examined three global analysis data sets of sea surface temperature (SST) in  
289 the Chinese coastal waters. For doing so, we have compared a number of statistical properties  
290 for 26 coastal hydrological locations as given by the analyses and by a newly digitized and  
291 homogenized data set (Li et al., 2018). For demonstrating the utility of the local data set,  
292 named LH in the following, we have compared the local SST series with independent local  
293 homogenized surface air temperature (SAT) data from nearby meteorological stations. The  
294 variations of the two series are fully consistent. Another argument alluding to the quality of  
295 the LA data set is that the differences between LH and the three LAs (localized data from the  
296 different global analyses) considered are not uniform (except for the time mean); instead the  
297 LAs deviate in different ways from LH. If this would not be the case, one could be tempted to  
298 argue that the differences are manifestations of inefficiencies of the LH data set. This is not  
299 the case.

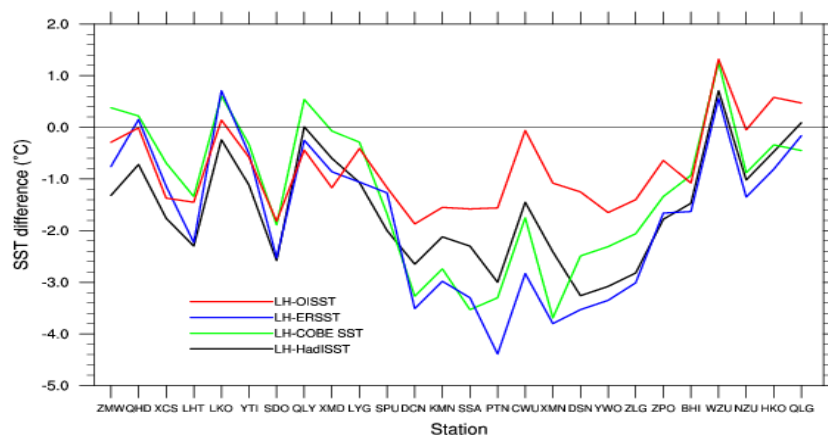


300 Our main results are:

- 301 – The mean SST in LH at many sites is considerably lower than that in the LA-data. We  
302 suggest that this is related to the coastal position of LH, and the averaging in the LA  
303 data. Consistent with this hypothesis is that the differences are largest in the case of  
304 the coarsest analysis (ERSST), but weakest in the OISST-data set with a resolution of  
305 a quarter of a resolution degree (Fig. 7) (Note that the difference LH minus LA-OISST  
306 is restricted to the warmer episode 1982-2015). However, systematic differences  
307 would not be expected to influence strongly the overall variability and trends.
- 308 – The first EOF in all data sets stands for a general warming, and the second for  
309 interannual variability. This is not only so in the local LH-data but also in all globally  
310 gridded-based LA-datasets.
- 311 – In the years following the introduction of satellites in monitoring SST, since about 1980,  
312 the different global analyses converge, and the differences to the local data set become  
313 smaller. In support of this, the comparison with the high resolution analysis OISST for  
314 the post-satellite time 1982-2014 reveals few differences (not shown, see Fig. SOM-4).
- 315 – In the years before 1980, some noteworthy differences are found. The differences  
316 between the LH-data anomalies and the LA-data anomalies are non-uniform across the  
317 different LA data sets. For instance, for ERSST the long-term trends differ, in case of  
318 COBE SST several jumps emerge, and in case of HadISST, a jump is found at the time  
319 of the advent of the routine satellite data, but also a trend in PC2 of the differences.

320 Thus, our overall conclusion is that the global gridded SST datasets correctly describe the  
321 main features of variabilities and trends in regional waters, but that significant improvements  
322 in the regional analyses may be gained when quality controlled homogenized data are  
323 incorporated. In particular for the time prior to the usage of remote sensing by satellites, and  
324 in regions where observational efforts have been limited, such efforts are valuable  
325 contributions to climate variability and change studies. Our example should also be an  
326 encouragement for national climate services to revisit regional data, and to invest into the  
327 elimination of inconsistencies caused by inhomogeneities.





328

329 **Figure 7.** The mean SST differences at the 26 locations between LH and LA-OISST (1982-2015; red  
330 line), LH and LA-ERSST (1960-2015; blue line), LH and LA-COBE SST (1960-2015; green line) and  
331 LH and LA-HadISST (1960-2015; black line)

332

333 *Acknowledgments.* The work is funded by the program of National Natural Science  
334 Foundation of China (No. 41376014; No. 41706020), the National Key Research and  
335 Development Program of China (No.2018YFA0605600; No. 2017YFC1404700) and also  
336 supported by the Hamburg University's Cluster of Excellence CliSAP in Germany.

337

### 338 **References**

- 339 Belkin, I. M.: Rapid warming of Large Marine Ecosystems, *Progr Oceanogr*, 81(2009),  
340 207-213, 2009.
- 341 Bungel, L. and Clarke, Allan J.: A verified estimation of the El Niño index Niño-3.4 since  
342 1877, *J. Climate*, 22(14), 3979-3992, 2009.
- 343 Harris, I., Jones, P. D., Osborn, T.J., and Lister, D.H.: Updated high-resolution grids of  
344 monthly climatic observations- the CRU TS3.10 dataset, *Int. J. Climatol.* 34, 623-642,  
345 2014.
- 346 Hiraharas, S., Ishii, M., and Fukuda, Y.: Centennial-Scale Sea Surface Temperature  
347 Analysis and Its Uncertainty, *J. Climate*, 27, 57-75, 2014.
- 348 Ishii, M., Shouji, A., Sugimoto, S., and Matsumoto, T.: Objective analyses of sea-surface  
349 temperature and marine meteorological variables for the 20th century using ICOADS  
350 and the Kobe Collection, *Int. J. Climatol.*, 25, 865-879, 2005.



- 351 Jin, Q. H. and Wang, H.: Multi-time scale variations of sea surface temperature in the China  
352 Seas based on the HadISST dataset, *Acta. Oceanol. Sin.*, 30, 14-23, 2011.
- 353 Kim, K.Y., North, G.R. and Huang, J.P.: EOFs of one dimensional cyclostationary time  
354 series: Computation, examples, and stochastic modeling, *J. Atmos. Sci.*, 53, 1007-1017,  
355 1996.
- 356 Li, Y., Wang, G.S., Fan, W.J., Liu, K.X., Wang, H., Tinz, B., von Storch, H., and Feng, J. L.:  
357 The homogeneity study of the sea surface temperature data along the coast of the China  
358 Seas, *Acta. Oceanol. Sin.* 40, 17-28, 2018 (in Chinese but with English abstract).
- 359 Liu, Q.Y. and Zhang, Q.: Analysis on long-term change of sea surface temperature in the  
360 China Seas, *J. Ocean University China* 12, 295-300, 2013.
- 361 Mantua, N.J. and Hare, S.R.: The Pacific decadal oscillation, *J. Oceanogr.*, 58, 35-44, 2002.
- 362 Rayner, N.A., Parker, D.E., Horton, E.B., and others: Global analyses of sea surface  
363 temperature, sea ice, and night marine air temperature since the late nineteenth century,  
364 *J. Geophys. Res.*, 108(D14),1063-1082, 2003.
- 365 Reynolds, R.W., Smith, T.M., Liu, C.Y., Chelton, D.B., Casey, K.S. and Schlax, M.: Daily  
366 high-resolution-blended analyses for sea surface temperature, *J. Climate*, 20, 5473-5496,  
367 2007.
- 368 Park, K. A., Lee, E.Y., Chang, E., and Hong, S.: Spatial and temporal variability of sea  
369 surface temperature and warming trends in the Yellow Sea. *J. Mar. Sys.* 143, 24-38,  
370 2015.
- 371 Saji, N. H., Goswami, B. N., Vinayachandran, P.N., Yamagata, T.: A dipole mode in the  
372 tropical Indian Ocean, *Nature* 401, 360-363, 1999.
- 373 Sen, P.K.: Estimates of regression coefficient based on Kendall's tau, *J. Am. Stat. Assoc.* 63,  
374 1379-1389, 1968
- 375 Smith, T.M., Reynolds, R.W., Peterson, T.C. and Lawrimore, J.: Improvements to NOAA's  
376 historical merged land-ocean surface temperature analysis (1880-2006), *J. Climate*,  
377 21(10), 2283-2296, 2008.
- 378 Tokinaga, H., Xie, S.P., Deser, C., Kosaka, Y. and Okumura, Y. M.: Slowdown of the  
379 Walker circulation driven by tropical Indo-Pacific warming, *Nature*, 491(7424), 439-43,  
380 2012.
- 381 Vecchiga, Clement, A., Soden, B.J.: Examining the Tropical Pacific's Response to Global  
382 Warming, *Eos Transactions American Geophys Union*, 89(9), 81-83, 2008.
- 383 Von Storch, H. and Zwiers, F.W.: Statistical analysis in climate research. Cambridge  
384 University Press: London, 1999.



- 385 Wu, L. X., Cai, W. J., Zhang, L.P., and others: Enhanced warming over the global  
386 subtropical west boundary currents, *Nat. Clim. Change*, 2(3), 161-166, 2012.
- 387 Xie, S.P., Clara, D., Gabriel, A. V., Ma, J., Teng, H.Y. and Andrew, T. W.: Global warming  
388 pattern formation: sea surface temperature and rainfall, *J. Climate*, 23(4), 966-986,  
389 2010.
- 390 Xu, W.H., Li, Q.X., Wang, X.L., Yang, S., Cao, L.J. and Feng, Y.: Homogenization of  
391 Chinese daily surface air temperature and analysis of trends in the extreme temperature  
392 indices, *J. Geophys. Res.*, 118(17), 9708-9720, 2013.
- 393 Yeh, S.W. and Kim, C. H.: Recent warming in the Yellow/East China Sea during winter and  
394 the associated atmospheric circulation, *Cont. Shelf Res.*, 30, 1428-1434, 2010.
- 395
- 396



### 397 **Appendix A: Consistency of homogenized SST data set with homogenized SAT data set**

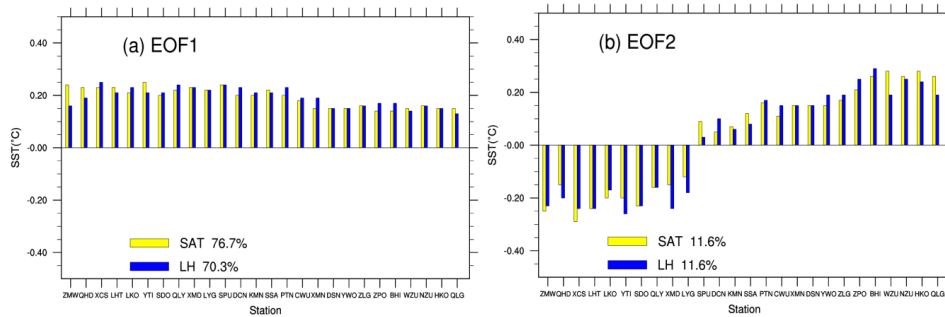
398 We examine if the SST data is consistent with other local homogenized data, specifically with  
399 time series of SAT at various locations along the Chinese coast. This data set contains data  
400 from many sites. For each of the SST measuring sites, there is at least one SAT stations within  
401 100 km distance. We select one such SAT station with higher correlation relationship with  
402 SST time series, and form 26 pairs of located SST/SAT data. However, we do not compare the  
403 SST and SAT data directly, but we derive for both times series empirical orthogonal functions  
404 (EOFs), and compare the patterns and the coefficient time series (PCs) of the two EOF sets  
405 (Fig. A1). It turns out that the patterns are similar. When compared to series drawn from the  
406 gridded CRU TS 3.24.01, we find a strong similarity (not shown, see Fig. SOM-1).

407 The first EOFs of SST and SAT *in site* describe an overall warming, with a slight tendency of  
408 stronger warming in terms of both SST and SAT in the northerly Bohai and Yellow Sea (Fig.  
409 A1a). This pattern is dominant, representing 70.3% and 76.7% of the total interannual  
410 variance. The warming is mostly continuous from about 1970 until 2010 (Fig. A1c). The  
411 similarity of the principal components – expressed by 0.97 in terms of the correlation  
412 coefficient – is striking (Fig. A1c). The second EOF (Fig. A1b) explains considerably less  
413 variance – namely about 11.6%. They describe a North-South contrast, and stationary PCs,  
414 varying around 0 without prolonged positive or negative excursions (Fig. A1d). Also the PCs  
415 of the second PCs of SST and SAT show a remarkably parallel development – with a high  
416 correlation of 0.86 (Figs.A1d). The PCs of SAT-CRU also show high correlations of 0.94 and  
417 0.83 with the SST *in site* (not shown, see Fig. SOM-1).

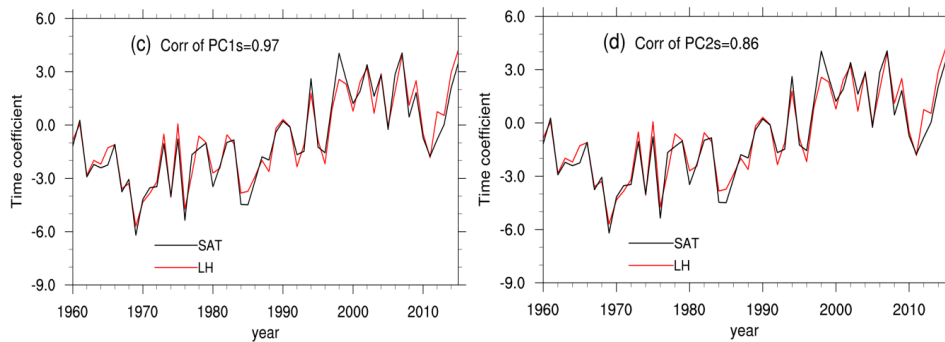
418 We conclude that the two data sets are consistent; the first EOFs describe the warming of the  
419 recent **decades of years**; the second EOFs describe interannual variability, and may be  
420 influenced by ENSO and other patterns of natural variability. We furthermore conclude that  
421 the new description of SST variability and trends at the 26 sites along the Chinese coast  
422 presents a reliable account of the past since 1960 – and thus may serve as a benchmark for  
423 assessing global analyses of SST datasets.



424



425



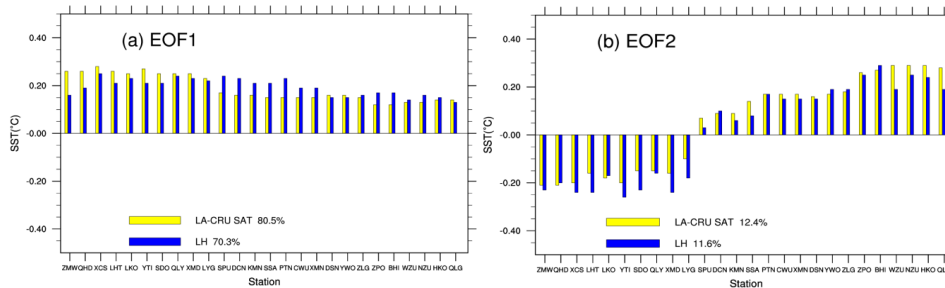
426 **Fig. A1.** Comparison of the EOF1 and EOF2 derived from the LH data set of local SST at 26 sites (blue  
 427 bars; red lines), and derived from the SAT at the same sites (yellow bars; black lines).  
 428 Top: EOF spatial patterns, bottom: principal components (time coefficients).

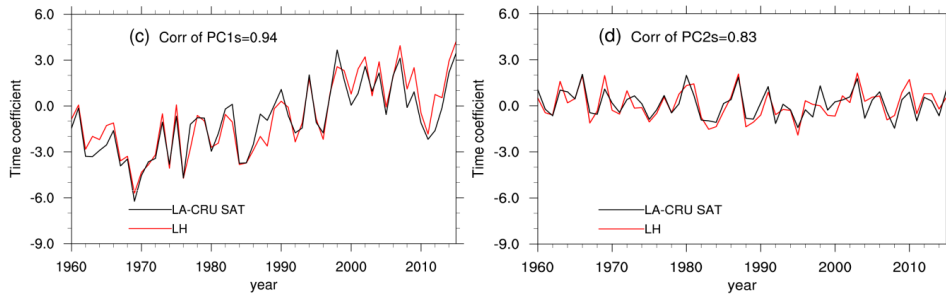
429

430

**Appendix B: Supplementary Online Material (SOM)**

431

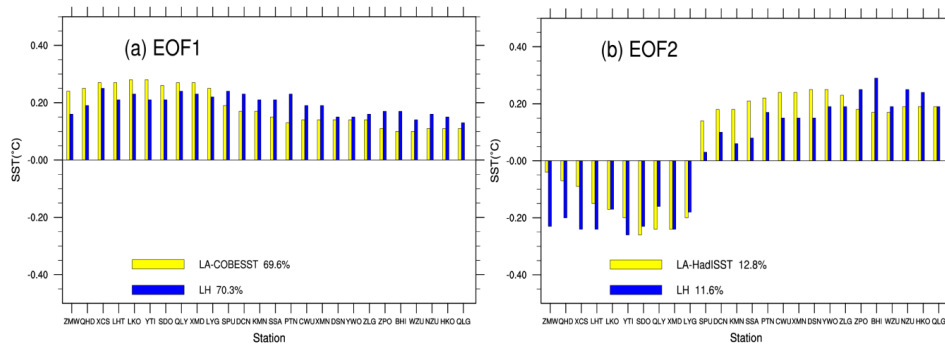




432

433 **Fig. SOM-1.** Comparison of the EOF1 and EOF2 derived from the LH data set of local SST at 26 sites  
 434 (blue bars; red lines), and derived from the CRU SAT at the same sites (yellow bars; black lines).  
 435 Top: EOF spatial patterns, bottom: principal components (time coefficients).

436



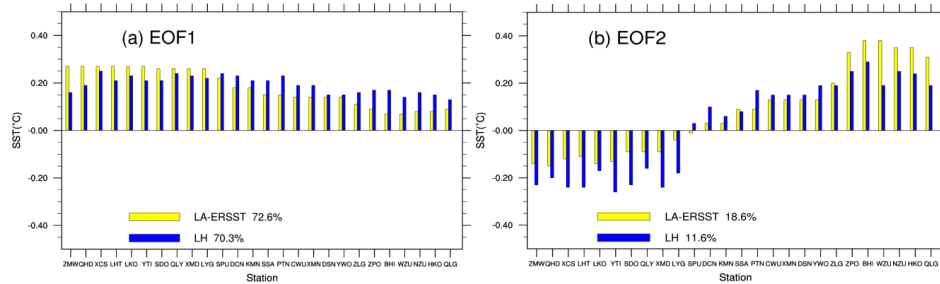
437

438 **Fig. SOM-2.** Comparison of the EOF1 and EOF2 derived from the LH data set of local SST at 26 sites  
 439 (blue bars; red lines), and derived from the localized analysis data LA-COBE SST (yellow bars; black  
 440 lines). Top: EOF spatial patterns, bottom: principal components (time coefficients).  
 441

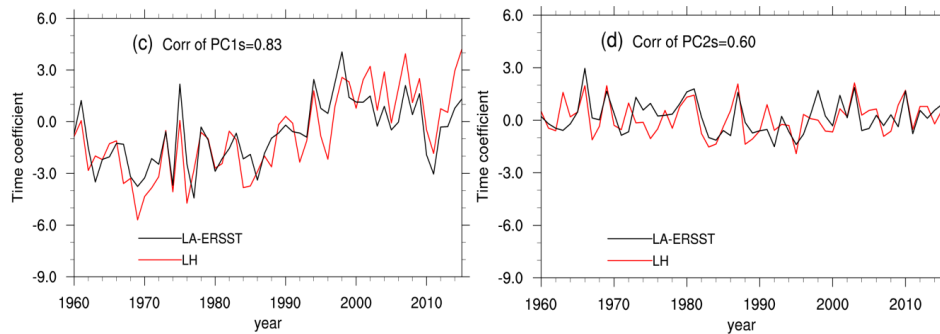
442



443



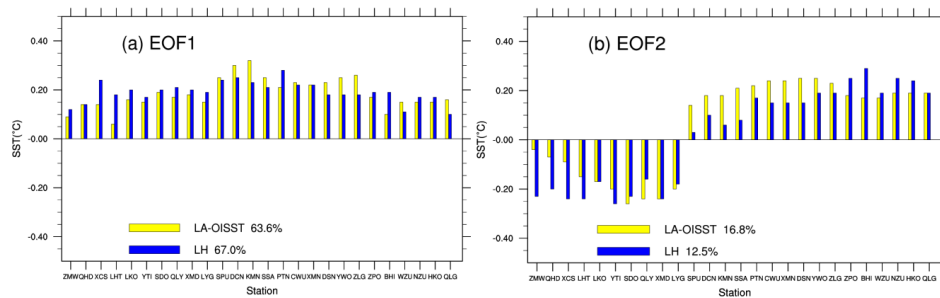
444



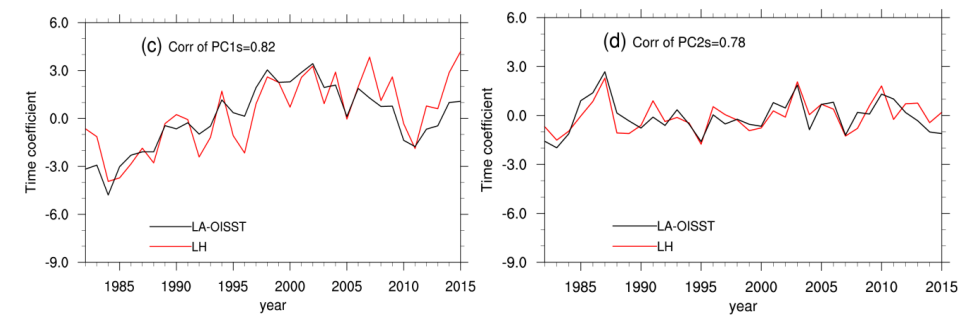
445 **Fig. SOM-3.** Comparison of the EOF1 and EOF2 derived from the LH data set of local SST at 26 sites  
 446 (blue bars; red lines), and derived from the localized analysis data LA-ERSST (yellow bars; black lines).  
 447 Top: EOF spatial patterns, bottom: principal components (time coefficients).

448

449



450





451 **Fig. SOM-4.** Comparison of the EOF1 and EOF2 derived from the LH data set of local SST at 26 sites  
452 (blue bars; red lines), and derived from the localized analysis data LA-OISST (yellow bars; black lines).  
453 Top: EOF spatial patterns, bottom: principal components (time coefficients).

454





455 Table SOM-1. Statistics of the time series of the localized SST-analysis (LA-COBE SST) data series at the  
 456 26 station, as well as the differences (Diff) between the pairs of time series. The correlation coefficients  
 457 between LH and LA-COBE SST are also calculated (the 90% confidence level is 0.22, without considering  
 458 serial correlation). Red numbers indicate that the correlation coefficients do not exceed the 90% confidence  
 459 level.

No	station	Mean LA-COBE SST	Diff	Std-dev LA-COBE SST	Diff	Trend ( °C/10yrs)	Diff	Corr
1	ZMW	11.13	0.38	0.52	0.01	0.17	0.00	0.60
2	QHD	11.99	0.22	0.54	0.04	0.16	0.10	0.56
3	XCS	12.23	-0.69	0.56	0.14	0.14	0.15	0.74
4	LHT	12.70	-1.34	0.59	0.00	0.10	0.11	0.59
5	LKO	12.75	0.61	0.60	-0.01	0.10	0.12	0.64
6	YTI	12.98	-0.33	0.61	-0.03	0.07	0.10	0.66
7	SDO	13.98	-1.89	0.61	-0.02	0.01	0.13	0.68
8	QLY	13.83	0.54	0.62	0.03	0.04	0.13	0.72
9	XMD	13.83	-0.07	0.62	0.01	0.03	0.19	0.55
10	LYG	15.14	-0.29	0.57	0.00	0.03	0.18	0.55
11	SPU	19.09	-1.68	0.45	0.20	0.18	0.08	0.77
12	DCN	20.94	-3.27	0.43	0.22	0.19	0.05	0.81
13	KMN	20.94	-2.74	0.43	0.13	0.19	-0.02	0.78
14	SSA	23.25	-3.53	0.38	0.22	0.20	0.01	0.82
15	PTN	23.29	-3.30	0.41	0.11	0.20	-0.01	0.79
16	CWU	23.29	-1.75	0.41	0.10	0.20	-0.03	0.85
17	XMN	22.90	-3.69	0.40	0.14	0.19	0.00	0.78
18	DSN	23.33	-2.49	0.41	0.04	0.21	-0.08	0.68
19	YWO	23.33	-2.31	0.41	0.02	0.21	-0.08	0.77
20	ZLG	24.49	-2.06	0.40	0.04	0.18	-0.03	0.81
21	ZPO	24.95	-1.34	0.33	0.17	0.11	0.07	0.80
22	BHI	24.53	-0.93	0.34	0.21	0.10	0.08	0.78
23	WZU	24.53	1.26	0.34	0.09	0.10	0.07	0.73
24	NZU	25.34	-0.88	0.35	0.14	0.12	0.04	0.77
25	HKO	25.34	-0.34	0.35	0.13	0.12	0.04	0.85
26	QLN	26.25	-0.45	0.36	0.08	0.13	0.05	0.68

460



461 Table SOM-2 Statistics of the time series of the localized SST-analysis (LA-ERSST) data series at the 26  
 462 station, as well as the differences (Diff) between the pairs of time series. The correlation coefficients  
 463 between LH and LA-ERSST are also calculated (the 90% confidence level is 0.22, without considering  
 464 serial correlation). Red numbers indicate that the correlation coefficients do not exceed the 90% confidence  
 465 level.

No	Station	Mean LA-ERSST	Diff	Std-dev LA-ERSST	Diff	Trend ( °C/10yrs)	Diff	Corr
1	ZMW	12.26	-0.76	0.53	0.00	0.16	0.01	0.69
2	QHD	12.06	0.15	0.55	0.03	0.17	0.09	0.70
3	XCS	12.68	-1.14	0.54	0.17	0.17	0.12	0.82
4	LHT	13.59	-2.23	0.52	0.07	0.16	0.05	0.78
5	LKO	12.65	0.71	0.54	0.05	0.16	0.06	0.77
6	YTI	13.16	-0.51	0.52	0.06	0.16	0.01	0.79
7	SDO	14.62	-2.53	0.50	0.09	0.14	0.00	0.76
8	QLY	14.62	-0.25	0.50	0.14	0.14	0.03	0.85
9	XMD	14.62	-0.86	0.50	0.12	0.14	0.08	0.78
10	LYG	15.92	-1.06	0.50	0.07	0.12	0.09	0.81
11	SPU	18.68	-1.27	0.46	0.19	0.10	0.16	0.65
12	DCN	21.18	-3.51	0.37	0.28	0.12	0.12	0.70
13	KMN	21.18	-2.98	0.37	0.19	0.12	0.05	0.71
14	SSA	24.37	-4.39	0.32	0.20	0.12	0.09	0.69
15	PTN	24.37	-2.83	0.32	0.19	0.11	0.08	0.75
16	CWU	23.02	-3.80	0.33	0.22	0.11	0.06	0.77
17	XMN	23.02	-3.30	0.33	0.28	0.12	0.07	0.71
18	DSN	24.37	-3.53	0.32	0.13	0.11	0.02	0.63
19	YWO	24.37	-3.35	0.32	0.12	0.11	0.02	0.65
20	ZLG	25.44	-3.01	0.31	0.13	0.09	0.06	0.67
21	ZPO	25.28	-1.66	0.35	0.14	0.04	0.14	0.56
22	BHI	25.23	-1.63	0.41	0.15	0.02	0.18	0.49
23	WZU	25.23	0.56	0.41	0.03	0.03	0.17	0.37
24	NZU	25.81	-1.35	0.37	0.12	0.01	0.16	0.54
25	HKO	25.81	-0.81	0.37	0.11	0.01	0.16	0.66
26	QLN	25.96	-0.16	0.34	0.10	0.05	0.13	0.47

466

467